Investigation and Monitoring of Antibody Aggregation in Biopharmaceutical Manufacturing

Mariana Medeira Silva Ressurreição
Mestrado Integrado em Engenharia Biológica

Abstract

In monoclonal antibody (mAb) manufacturing, protein aggregates are one of the most relevant critical quality attributes and their levels must be controlled thoroughly. This work focuses both on understanding the mechanism of aggregation and the assessment of Raman spectroscopy as a tool for online aggregate quantification. To that end, two mAbs were investigated. First, aggregation behaviour during and after temporary exposure to acidic pH was studied to learn what promotes aggregation during low pH virus inactivation step in downstream processing (DSP). Electrostatic repulsion between antibody molecules prevents mAb coagulation at pH values between 2.5 and 3.5 and low ionic strength. Formation of aggregates occurs during and after neutralization to higher pH and ionic strength values. Further, the ability to quantify antibody aggregates with Raman technology for monitoring and control was tested. Smoothing techniques for spectral data such as Wavelet transform and Empirical Mode Decomposition were investigated and compared to Savitzky-Golay, providing better results. Prediction of monomer concentration with a PLS model under process relevant ranges was achieved with good results. Although aggregates were not successfully quantified in process relevant ranges, information in increased ranges was decently predicted with a regression model. This lays the foundation towards online monitoring of aggregate concentration.

1. Introduction

One of the most important critical quality attributes (CQA) in antibody manufacturing are the aggregate forms of the product. Under the scope of continuous processing, it's monitoring and control in real time is of extreme importance.

Antibody Aggregation in Downstream Processing

The most common and significant source of aggregate formation in DSP is the virus inactivation (VI) step [1]. When incubated at low pH, proteins tend to denature, *i.e.* alter their conformation, which leads to exposure of hydrophobic residues previously buried within the protein's interior. If (partially) denatured protein molecules are unable or slow to refold back to their native conformation afterwards, hydrophobic side chains of different protein molecules may interact, leading to formation of dimers and higher order oligomers [2]. For successful assembly of fully continuous DSP, profound knowledge about each unit operation is critical. Regarding low pH VI, the impact of process parameters on antibody stability and aggregation behaviour merit further investigation for potential reduction of product loss.

The two key process parameters in VI are undoubtedly duration and selected pH. On one hand, the process must to be long enough to achieve robust virus reduction, and, on the other, the longer the incubation at low pH, the higher the risk of product loss [3]. The pH of incubation, must be below 4 to guarantee the destruction of the lipid envelopes of the viruses but the process value will depend on the aimed viral clearance. Concerning the effect on the product, acidic pH will dictate the distribution of surface charges on proteins, affecting intra and intermolecular protein-protein interactions. At extreme values, proteins are heavily charged

and a dense charge population on the proteins' surfaces can significantly increase repulsive interactions, leading to at least partial unfolding. Aggregation under these conditions will depend on the relative contribution of inter-molecular hydrophobic attraction and electrostatic repulsion [4]. Strongly related to pH is ionic strength of the protein solution. Ions in solution will interact with the proteins, leading to altered charge-charge interactions and possibly different behaviour of aggregation [4].

Application of Raman Spectroscopy for monitoring and control of mAb Aggregates

Spectroscopic methods have been widely used as tools for structural analysis of therapeutic proteins in DSP [5]. Nevertheless, the application of Raman spectroscopy has not yet been reported in literature. Raman spectroscopy is a vibrational spectroscopic technique based on the inelastic scattering of photons, also known as Raman effect [6]. It measures changes in the scattered light frequencies between molecule's ground and excited vibrational states when they are interacting with a beam of light, resulting in a Raman spectrum containing bands correspondent to molecular configuration [7]. It offers several advantages when compared to other analytical techniques: (i) no two different molecules present the exact same spectrum; (ii) it is non-destructive; (iii) its operational wavelength is independent of vibrational modes and can be used in ranges from UV to near-infrared; (iv) water, the natural medium for protein, is a weak Raman scatterer, and does not interfere significantly; (v) does not require large samples or extensive preparation and the spectra can be obtained in many physical states. Nevertheless, Raman is a very weak physical phenomenon, as very few photons in the millions that interact with the molecules will present Raman scattering. Additionally, in the visible region, fluorescence emitted from the sample has a quantum yield much higher than that of Raman scattering, overwhelming its signal [7].

2. Materials and Methods

MAb-1 was expressed by Chinese hamster ovary cells inside a perfusion bioreactor. Cell-free harvest was purified by protein A affinity chromatography. The eluate was immediately neutralized using 1 M Tris-HCl pH 8.0 buffer solution and stored in the fridge prior to use. MAb-2 was provided as neutralized protein A eluate.

The chemicals used for the formulation of buffer solutions were sodium phosphate (Sigma-Adrich, USA), L-arginine (Sigma, USA), sodium azide (Sigma-Adrich, USA), citric acid (Fluka Analytical, Switzerland), trisodium citrate (Sigma-Aldrich, USA), sodium chloride (Sigma-Aldrich, USA) and sodium hydroxide (Sigma-Aldrich, USA) and 8-Anilino-1-naphthalenesulfonic acid (ACROS ORGANICS, Belgium).

Aggregation and Unfolding Studies at Low pH

Dynamic Light Scattering Measurements

Average hydrodynamic size of the protein during incubation at low pH was measured over the course of one hour by means of *in-situ* dynamic light scattering using a Malvern ZetaSizer Nano ZS instrument (Malvern, UK) equipped with a 633 nm He-Ne and detection at 173° scattering angle. All measurements were conducted at 25 °C.

ANS Fluorescence Measurements

Fluorescence of the dye 1-anilinonaphthalene-8- sulfonate (ANS) in presence of either mAb was measured on a PerkinElmer EnSpire 2300 Multilabel Reader instrument (PerkinElmer, USA). Emission was recorded at 490 nm upon excitation at 403 nm. Sample preparation was identical to that for DLS measurements. Only differences were that fluorescence measurements were conducted at 0.25 g/L mAb concentration and ANS was added at a 1:10 (mAb:ANS) molar ratio. Immediately after preparation, 250 µL of sample were transferred into a well of a Greiner Bio-One µClear non-binding black 96 well plate (Greiner Bio-One, Germany) and the measurement was started.

Aggregation Studies for Neutralized Solutions after Temporary Exposure to Low pH

Size-exclusion Chromatography Coupled to Multi-angle Light Scattering

Neutralized solutions were also analysed by SEC-MALS using a Superdex 200 10/300 GL size-exclusion column (GE Healthcare, USA) connected to an Agilent 1200 series HPLC system (Agilent Technologies, USA), consisting of quaternary pump, auto-sampler and UV absorbance detector. 50 µL of sample were injected into the column and eluted for 60 minutes at a constant flow rate of 0.5 mL/min using 100 mM sodium phosphate pH 7.0, 200 mM L-arginine and 1 g/L sodium azide as mobile phase. UV absorbance of the effluent was recorded at 280 nm wavelength. Injections were made initially after neutralization and repeated once per hour, for 10 hours. Further, static light scattering (SLS) from the liquid leaving the column was measured using a DAWN HELEOS-II multi-angle light scattering device (Wyatt Technology, USA) Agilent ChemStation (Agilent Technologies, USA) and Wyatt Astra V (Wyatt Technology, USA) software was used for analysis of UV absorbance and light scattering data, respectively.

Raman Spectra Measurement and Analysis

Raman spectra of protein aqueous solutions were acquired using a RamanRxn2 Multi-channel Raman Analyzer (Kaiser Optical Systems, Inc., USA). The spectrometer is equipped with a Charge Coupled Device (CCD) detector, a HPG-785 grating and an excitation laser at 785 nm wavelength and 1 cm^{-1} of spectral resolution. Each spectrum was measured from 100 to 3425 cm^{-1}. The laser power employed for the measurements was 400 W. All data was collected in iC Raman 4.1.917.0 SP2 software (Mettler Toledo & Kaiser Optical Systems, Inc., USA) and processed and analysed using Matlab 8.6.0. software.

Data Analysis

For the PLS regression model, 80% of the data set was used for the training and cross-validation (CV) of the model and the remaining 20% were used for its validation. For a greater confidence in the RMSEP, a rotation procedure was implemented. In each rotation, 5 in total, different measurements were assigned to the external predicted set. Additionally, the measurements assigned for the prediction set were evenly distributed between the ranges of the to-be-predicted variables. Resorting to this method, from each model one receives five distinct results, one for each rotation.

Before calibration, the spectra were pre-treated with a pre-determined technique selected for smoothing, then Standard Normal Variate

normalization and mean centering. After pre-treatment, the extremes of the spectra, below 450 and above 3100 cm^{-1}, were cut, as it was known that no information would come from these regions. Moreover, two short regions known to be affected by the laser according to the Raman device manufacturer were also cut: 1820 – 1880 and 2530 – 2590 cm^{-1}.

The optimal number of latent variables (LV) was determined by the lowest relative root mean square error in CV (relRMSECV). RMSE is given by equation (1), where N is the total amount of samples, $y_{ref,I}$ is the reference value given by an analytical measurement and $y_{pred,I}$ is the value predicted from the Raman spectrum of the samples using the regression model.

$$RMSE = \sqrt{\frac{\sum_{i=1}^{N}\left(y_{ref,i}-y_{pred,i}\right)^2}{N}} \quad (1)$$

The relative root mean square error in prediction is obtained by dividing the RMSE by the range of the prediction set.

The coefficient of determination, Q^2, for the validation phase, reveals how much of the variance of the Y (monomer or aggregate concentration) is explained by the independent variable (the spectra). It is determined by the quotient of explained variance in the model (SSE) by total variance in the data set (SST). In a perfect correlation between observed and predicted values, it equals 1. SSE and SST are given by equations (2) and (3), respectively.

$$SSE = \sum_{i=1}^{N}(y_{ref,i}-y_{pred,i})^2 \quad (2)$$

$$SST = \sum_{i=1}^{N}(y_{ref,i}-\overline{y_{ref}})^2 \quad (3)$$

3. Results and Discussion

Characterization of Antibody Aggregation

Aggregation Studies at Low pH

Aggregation behaviour of 1 g/L mAb solutions in 50 mM sodium citrate at pH 2.5, 3.0 and 3.5 and at fixed ionic strength of 50 mM was determined by *in-situ* DLS. Figure 1 shows the evolution of the average hydrodynamic radius (<R_h>) for both antibodies as a function of time and solution pH. Over the course of 1 hour, hydrodynamic size of mAb-1 and mAb-2 remains constant within statistical uncertainty, indicating that no significant aggregation is occurring under acidic conditions at low ionic strength.

The undetectable aggregate formation at low pH could be explained by the dominant contribution of repulsive electrostatic interactions over any other type of attractive intermolecular interaction, preventing mAb

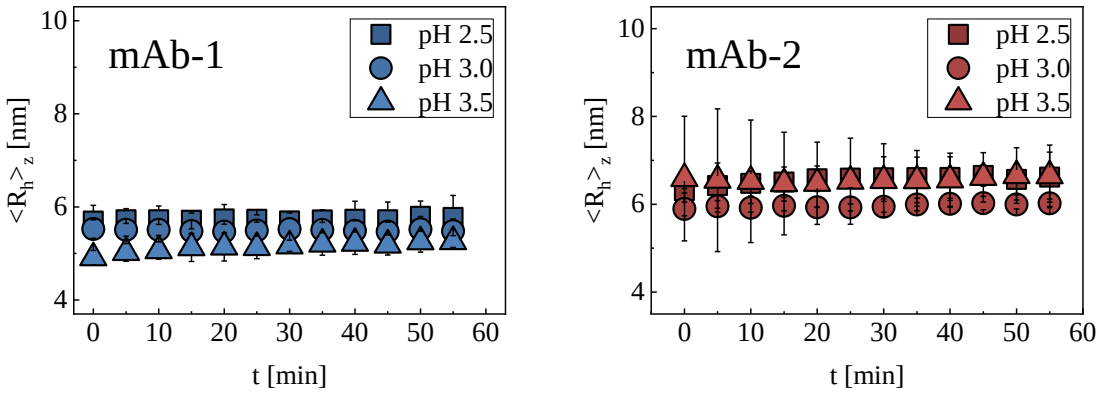

Figure 1 – Time evolution of the average hydrodynamic radius of 1 g/L mAb-1 (left) and mAb-2 (right) solutions in 50 mM sodium citrate at pH 2.5 (square), 3.0 (circle) and 3.5 (triangle) with total ionic strength fixed at 50 mM. Error bars represent 90% confidence intervals for the mean, which was calculated by averaging results from three independent measurements.

molecules from forming oligomers. Under acidic conditions, far from the antibodies' isoelectric point (pI), polypeptide chains are highly protonated and thus will strongly repel each other by charge-charge interactions.

Protein Unfolding Studies at Low pH

Figure 2 shows the time evolution of the fluorescence intensity of 0.25 g/L mAb-1 and mAb-2 solutions at pH 2.5, 3.0, and 3.5 with 50 mM buffer molarity and 50 mM ionic strength. For mAb-1, measured fluorescence intensity remains virtually constant over the course of one hour, when the protein is incubated at pH 2.5 and 3.0. On the other hand, when mAb-1 is exposed to pH 3.5, fluorescence intensity increases gradually and almost reaches the level observed for pH 2.5 and 3.0 after one hour. Fluorescence intensity of ANS strongly increases when interacting with hydrophobic environments [29]. Since changes in protein surface hydrophobicity are commonly associated with conformational rearrangements, it can be concluded that a new conformational equilibrium is reached very fast when pH is lowered to 2.5 or 3.0 for mAb-1. In contrast, conformational changes occur much slower at pH 3.5, which would account for the increase of fluorescence intensity over time, as more hydrophobic binding sites are gradually made available for ANS molecules.

Figure 2 also contains the results for mAb-2 under otherwise identical conditions. At pH 2.5, fluorescence intensity increases substantially as function of time over the course of one hour. When mAb-2 is incubated at pH 3.0, fluorescence intensity remains almost constant at a level slightly lower than that observed for pH 2.5 immediately at the beginning. Further increasing solution pH to 3.5 again changes both qualitative and quantitative behaviour of fluorescence intensity as function of time. It starts from a comparatively low level and gradually increases over the course of one hour but never reaching the value observed for pH 3.0. Along the line of argument presented above, conformational dynamics of mAb-2 in response to exposure to an acidic pH of either 2.5 or 3.5 seem to happen on time-scales comparable to those relevant for viral inactivation in therapeutic antibody manufacturing. On the other hand, conformational steady state seems to be reached almost instantaneously at the intermediate pH of 3.0.

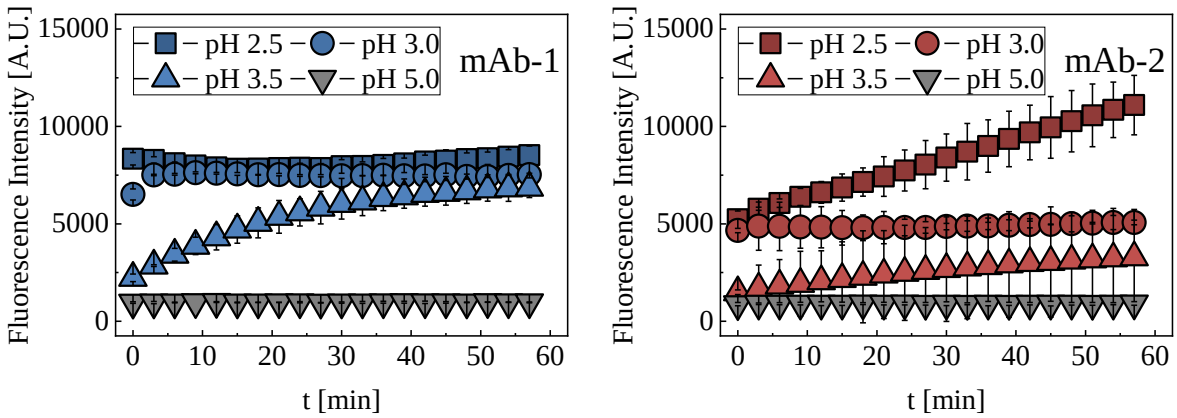

Figure 2 - Time evolution of fluorescence intensity of 0.25 g/L mAb-1 (left) and mAb-2 (right) solutions in 50 mM sodium citrate with I equal to 50 mM. ANS was added to the solutions in ten-fold molar excess with respect to the protein. Error bars represent 90% confidence intervals for the mean, which was calculated by averaging results from three independent measurements.

Aggregation Studies Following Neutralization after Temporary Exposure to Low pH

The results presented above suggest that at low pH, mAbs denature partially due to strong intra-molecular electrostatic repulsion. Simultaneously, inter-molecular charge-charge repulsion prevents oligomerization. The effect of a subsequent increase in pH was then studied systematically to understand how it may lead to formation of mAb aggregates during the VI step. Figure 1 contains the set of performed experiments. The final pH and ionic strength were always 5.0 and 100 mM, respectively. MAb solutions were analysed over the course of many hours after neutralization.

Table 1 - Conditions investigated for the study of antibody aggregation induced by pH-shift stress. The antibodies were incubation in 50 mM sodium citrate and 50 mM ionic strength, and, at the end of low pH incubation, solutions were always neutralized to pH 5.0 and 100 mM ionic strength. Solution pH was within ± 0.1 of target for all conditions.

pH [-]	Duration [min]
2.5	20
	40
	60
3.0	20
	40
	60
3.5	20
	40
	60

Figure 3 sums up the evolution of monomer content after neutralization for mAb-1 in all conditions presented in **Error! Reference source not found.**. It drops significantly within the first hour after neutralization for all investigated pHs and incubation times. Further, mild increase in monomeric fraction is detected after the third hour. Regarding the effect of pH, the measured monomer fraction after neutralization is smaller at every time point for pH 2.5 and 3.0 compared to pH 3.5. At pH 3.5, fraction of residual monomer is never below 70%, whereas at pH 2.5 and 3.0 it decreases to approximately 50%.

For mAb-2, results are presented in Figure 4. The monomer content decreases monotonically as a function of time after neutralization. Overall, aggregation behaviour is similar to that of mAb- 1. However, a few differences must be acknowledged: (i) the extent of aggregation after neutralization when mAb-2 is incubated at pH 3.5 is very small, while in the case of mAb-1 there is an evident decrease in monomer content; (ii) monomer loss in the first hours happens at a slower pace for mAb-2 than for mAb-1; (iii) while for mAb-1 a small increase in monomer content could be observed in the last hours, for mAb-2 monomer content is decreasing throughout the analysis. Important to mention, protein mass recovery in chromatographic analysis was complete for both mAbs and all conditions.

Concerning the impact of incubation time, in the case of mAb-1, for both pH 2.5 and 3.0 no noteworthy difference in the evolution of monomer fraction can be detected between incubation for 20, 40 or 60 minutes. Only for pH 3.5, the extent of monomer loss at a given time after neutralization has a dependence on incubation time. In the case of mAb-2, incubation time has limited impact on aggregation behaviour after neutralization for all conditions. Only for pH 3.5, the extent of monomer loss at a given time after neutralization has slight dependence on incubation time at low pH, but due to the very small amount of aggregation observed for that pH, differences are not statistically significant.

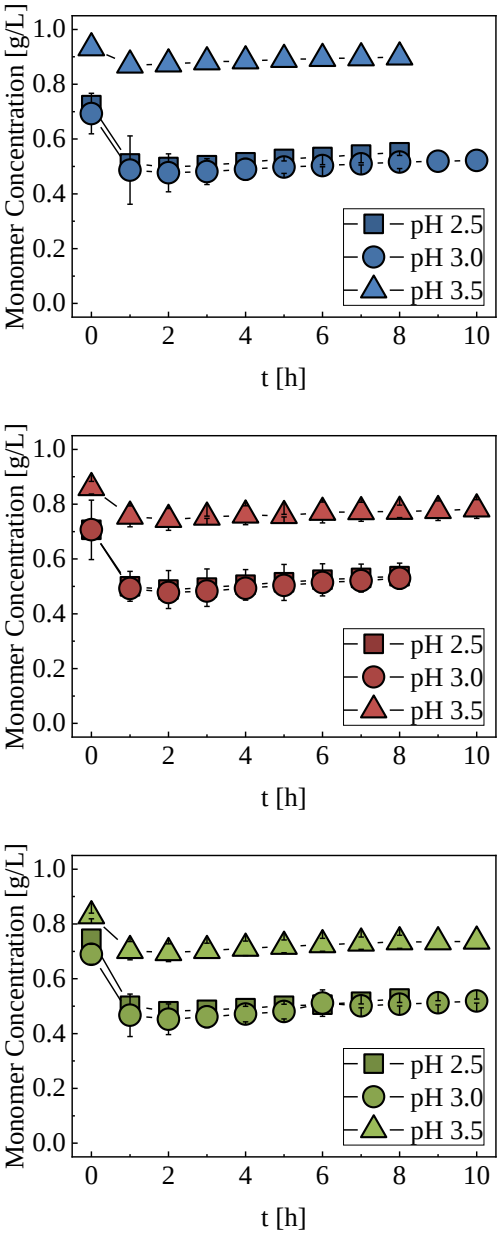

Figure 3: Monomer content as a function of time through the analysis by SEC obtained for 1 g/L mAb-1 solutions after neutralization to pH 5.0 and 100 mM ionic strength. Prior to neutralization, the protein was incubated at pH 2.5 (squares), 3.0 (circles) and 3.5 (triangles). Each row represents a different incubation time: upper row – 20 minutes; middle row – 40 minutes; lower row – 60 minutes. Error bars: 90% confidence intervals for the mean.

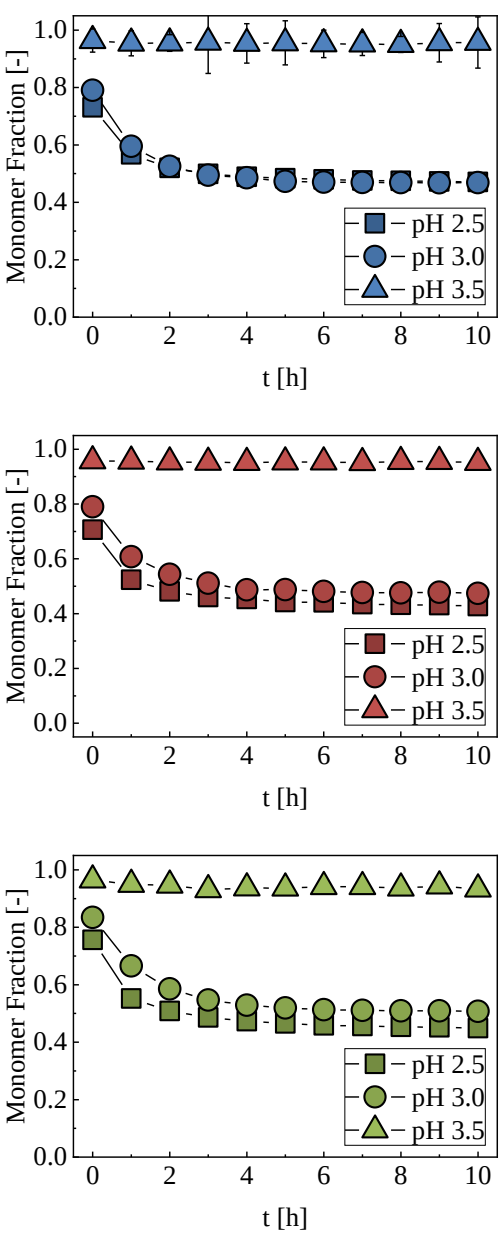

Figure 4: Monomer content as a function of time through the analysis by SEC obtained for 1 g/L mAb-2 solutions after neutralization to pH 5.0 and 100 mM ionic strength. Prior to neutralization, the protein was incubated at pH 2.5 (squares), 3.0 (circles) and 3.5 (triangles). Each row represents a different incubation time: upper row – 20 minutes; middle row – 40 minutes; lower row – 60 minutes. Error bars: 90% confidence intervals for the mean.

Assessment of Raman Spectroscopy as a Tool for Monitoring and Control

Data Acquisition

Multiple samples were generated by mixture of appropriate volumes of original protein stock solutions of different antibody concentration and aggregate content. Raman spectra of each sample was then acquired and a regression model was built to try to predict the monomer and aggregate concentration in each. In a first experiment, both mAbs were tested within a broad range of antibody aggregate content. Then, the experiment was repeated for mAb-2 with a set of samples representing a narrower and more realistic range of aggregate content. High aggregate concentration was met by inducing pH-shift stress on the molecules. To make sure the buffer molarity was identical in all original stocks, the stocks of low aggregate concentration were prepared by diluting the antibodies to the conditions of neutralization of the high content ones. For reference values, all samples were analysed by SEC.

Data Analysis

Data analysis of the acquired spectra was performed with PLS. To make sure the best results were obtained once calibrating the regression model, different techniques were tested for smoothing of the data, namely, Savitzky-Golay filter with and without the derivative function, Wavelet transform (WT) [8]–[10], Fourier transform (FT) [11] [12] and Empirical Mode Decomposition (EMD) with and without background removal (BR) [13]. All techniques were applied to the same data set in Matlab and their performance was tested both on the prediction of monomer and aggregate concentration. Table 2 presents the root mean square error in prediction (RMSEP) after application of each technique to the data set and the calibration of a PLS model.

Table 2 - Minimum RMSEP values for aggregate and monomer prediction of mAb-2 long-range aggregate content experiment by each of the tested techniques.

Technique	**RMSEP of aggregate concentration [g/L]**	**RMSEP of monomer concentration [g/L]**
SG	0.171	0.216
SG w/o derivative	0.147	0.129
FT	0.142	0.125
WT	0.140	0.106
EMD	0.563	0.892
EMD w/o BR	0.121	0.147

Upon comparison and selection of the best technique for each case, a PLS regression model was built for each data set. **Error! Reference source not found.** presents the average result obtained from the 5 rotations for the prediction of mAb-1 and mAb-2 monomer and aggregate concentrations. Concerning the results obtained for mAb-1, the regression model for the prediction of monomer concentration presents a relative root mean square error in prediction (relRMSEP) of 35%, which translates in a RMSEP of 0.942 g/L in a range between 0.536 and 3.81 g/L. As for the regression model calibrated for the prediction of aggregate concentration, a relRMSEP of 21% was obtained, reflecting a RMSEP of 0.471 g/L in a concentration range between 0.0145 and 2.63 g/L. It may be concluded that the prediction of neither monomer nor aggregate mAb-1 was successful. A prediction model with error above 20% is not suitable for monitoring of either monomer or aggregates in DSP. Regarding the results from mAb-2 in the same broad-range of

aggregate content experiment, prediction of monomer concentration presented a relRMSEP of 3.5%, expressing a RMSEP of 0.106 g/L in a concentration range between 0.437 and 3.76 g/L. For aggregate prediction, the regression model presents a relRMSEP of 7.51%, with a RMSEP of 0.121 g/L in a range between 0.0189 and 2.13 g/L. One can thus say that the PLS model predictions were both quite good for mAb-2 and both variables were decently predicted. Additionally, a Q^2 above 90% in both cases translates the ability of the models to successfully explain the variance in the spectral data. This presents a first proof of concept that Raman spectroscopy can be applied for aggregate prediction. Comparing both antibodies, mAb-2 clearly presents more promising results, but it must be taken into account the size of the data set used for each. Due to the removal of outliers, mAb-1's data set lost a considerable number of samples. In other words, it lost valuable information that could have improved the model.

For the prediction of monomer and aggregate concentration of mAb-2 in a short-range of aggregate content, the PLS model once again predicts monomer concentration quite accurately, with a relRMSEP of 6%, translated in a RMSEP of 0.146 g/L in a range between 1.69 and 4.45 g/L. However, for the prediction of aggregate concentration, the model presents a relRMSEP of 25%, reflecting a RMSEP of 0.113 g/L in a range between 0.0527 and 0.581 g/L. It appears that, under this range, Raman is not suitable for the quantification of aggregates. Nevertheless, the prediction capability of mAb-2 monomer is quite good.

4. Final Remarks

Overall, substantial evidence has been collected suggesting that mAb aggregation does not occur during the low pH hold but only after sharply raising pH. MAbs rapidly form aggregates upon neutralization and subsequently the aggregation rate decreases over the course of several hours. This can be explained by strong electrostatic repulsion between mAb molecules at low pH, which prevents self-association. Nevertheless, mAb molecules (partially) denature/unfold under those conditions. When pH and ionic strength

Table 3 - PLS prediction results of aggregate and monomer concentration for both mAb-1 and mAb-2.

	Predicted Variable	**N° of Samples**	**Calibration Range [g/L]**	**Prediction Range [g/L]**	**LV**	**Q^2**	**RMSEP [g/L]**	**rel RMSEP**
mAb-1	Monomer concentration	18	0.536-3.81	0.536-3.81	4	-0.573	0.942	0.345
	Aggregate concentration		0.0145-2.63	0.0145-2.634	6	0.471	0.424	0.205
mAb-2 broad range	Monomer concentration	24	0.437-3.76	0.437-3.76	14	0.964	0.106	0.0350
	Aggregate concentration		0.0189-2.13	0.0189-2.13	14	0.913	0.121	0.0751
mAb-2 narrow range	Monomer concentration	28	1.69-4.45	1.69-4.45	12	0.875	0.1462	0.0605
	Aggregate concentration		0.0527-0.581	0.0527-0.581	2	-0.112	0.113	0.254

are increased afterwards, repulsion is reduced and denatured mAb molecules can start to aggregate.

Regarding the ability to predict antibody aggregates with Raman spectroscopy, it was concluded that it was possible under a broad-range of aggregate content samples. With a relRMSEP of 7.5%, one can say the regression model was successful in predicting mAb-2 aggregates' concentration. Nevertheless, when shortening the aggregate content range of the samples, the error in prediction is not acceptable anymore. As for the prediction of mAb-2 monomer concentration, the regression models were successful in every experiment, with a relRMSEP always below 10%. The bad prediction results obtained for mAb-1 may be related to the short number of samples used in the data set for the training of the model. As a conclusion, this work provides the proof of concept that Raman spectroscopy is able to access antibody aggregate information. However, further intensive optimisations need to be exercised to allow the application of this technique in more realistic aggregate ranges, common in the DSP of antibody manufacturing.

5. References

[1] B. Somasundaram, K. Pleitt, E. Shave, K. Baker, and L. H. L. Lua, "Progression of continuous downstream processing of monoclonal antibodies: current trends and challenges," *Biotechnol. Bioeng.*, pp. 0–2, 2018.

[2] T. Chen, "Formulation concerns of protein drugs," *Drug Dev. Ind. Pharm.*, vol. 18, no. 11–12, pp. 1311–1354, 1992.

[3] S. Klutz, M. Lobedann, C. Bramsiepe, and G. Schembecker, "Continuous viral inactivation at low pH value in antibody manufacturing," *Chem. Eng. Process. Process Intensif.*, vol. 102, pp. 88–101, 2016.

[4] W. Wang, S. Nema, and D. Teagarden, "Protein aggregation-Pathways and influencing factors," *Int. J. Pharm.*, vol. 390, no. 2, pp. 89–99, 2010.

[5] M. Rüdt, T. Briskot, and J. Hubbuch, "Advances in downstream processing of biologics--Spectroscopy: An emerging process analytical technology," *J. Chromatogr. A*, vol. 1490, pp. 2–9, 2017.

[6] F. León-Bejarano, M. Ramírez-Elías, M. O. Mendez, G. Dorantes-Méndez, M. D. C. Rodríguez-Aranda, and A. Alba, "Denoising of Raman spectroscopy for biological samples based on empirical mode decomposition," *Int. J. Mod. Phys. C*, vol. 28, no. 9, 2017.

[7] Z.-Q. Wen, "Raman Spectroscopy of Potein Pharmaceuticals," *Wiley Intersci.*, 2006.

[8] P. M. Ramos and I. Ruisánchez, "Noise and background removal in Raman spectra of ancient pigments using wavelet transform," *J. Raman Spectrosc.*, vol. 36, no. 9, pp. 848–856, Sep. 2005.

[9] F. Ehrentreich and L. Summchen, "Spike removal and denoising of Raman spectra by wavelet transform methods," *Anal. Chem.*, vol. 73, no. 17, pp. 4364–4373, 2001.

[10] Y. Hu, T. Jiang, A. Shen, W. Li, X. Wang, and J. Hu, "A background elimination method based on wavelet transform for Raman spectra," *Chemom. Intell. Lab. Syst.*, vol. 85, no. 1, pp. 94–101, 2007.

[11] E. L. Kosarev and E. Pantos, "Optimal smoothing of 'noisy' data by fast Fourier transform," *J. Phys. E.*, vol. 16, no. 6, pp. 537–543, Jun. 1983.

[12] J. K. Kauppinen, D. J. Moffatt, H. H. Mantsch, and D. G. Cameron, "Smoothing of spectral data in the Fourier domain.," *Appl. Opt.*, vol.

21, no. 10, pp. 1866–72, 1982.

[13] N. E. Huang *et al.*, “The empirical mode decomposition and the Hilbert spectrum for nonlinear and non-stationary time series analysis,” *Proc. R. Soc. A Math. Phys. Eng. Sci.*, vol. 454, no. 1971, pp. 903–995, Mar. 1998.